ELSEVIER

Journal of Chromatography A, 796 (1998) 229–238

JOURNAL OF CHROMATOGRAPHY A

Electrostatic effects on protein partitioning in size-exclusion chromatography and membrane ultrafiltration

Narahari S. Pujar, Andrew L. Zydney*

Department of Chemical Engineering, University of Delaware, Newark, DE 19716, USA

Received 1 July 1997; received in revised form 19 September 1997; accepted 25 September 1997

Abstract

Although size-exclusion chromatography and membrane ultrafiltration are generally viewed as size-based separation processes, there is considerable evidence for the importance of electrostatic interactions. Experimental studies of size-exclusion chromatography and membrane ultrafiltration were performed in parallel using both neutral dextrans and charged proteins. Data for protein retention time and membrane sieving clearly indicate that the effective protein size increases with decreasing ionic strength due to the reduction in electrostatic shielding. These results were quantified using available theoretical models for the partitioning of charged solutes. The data clearly demonstrate the similarity of the electrostatic interactions and partitioning effects in size-exclusion chromatography and membrane ultrafiltration. © 1998 Elsevier Science B.V.

Keywords: Membrane ultrafiltration; Electrostatic interactions; Electric double layer; Proteins; Albumin

1. Introduction

Size-exclusion (or gel permeation) chromatography (SEC) and membrane ultrafiltration (UF) have generally been viewed as 'size-based' separation processes. There is, however, extensive experimental evidence that the separation characteristics of both SEC and UF can be strongly influenced by long-range, in particular electrostatic, interactions. In chromatographic systems, these interactions are often described as 'non-ideal' SEC since the separation characteristics are determined by electrostatic and/or hydrophobic interactions in addition to simple size differences [1]. For example, Potschka [2] showed that the myoglobin retention volume in a TSK 5000PW-3 column at pH 8.0 decreased from 19.1 to 16.3 ml as the ionic strength was reduced from 190 to 1 m*M* but the retention volume actually increased from 19.6 to 22.5 ml at pH 6.6 over a similar range of ionic strength. Pujar and Zydney [3] showed even more dramatic effects on albumin transport through a polyethersulfone ultrafiltration membrane, with the protein transmission (or sieving coefficient) decreasing by more than two orders of magnitude as the solution ionic strength was reduced from 150 to 1.5 m*M*.

There has been considerable debate in the literature over the actual physical origin of the ionic effects seen in SEC and UF systems [3,4]. Previous studies have attributed the observed behavior to: (1) changes in protein conformation or degree of aggregation, (2) alterations in the pore size characteristics of the resin (or membrane) due to intramolecular electrostatic interactions (e.g., swelling), (3) protein

*Corresponding author.

0021-9673/98/$19.00
PII S0021-9673(97)01003-0

adsorption onto or within the porous resin or membrane (possibly attributable to an ion-exchange-type process), and (4) protein exclusion from the porous resin or membrane due to intermolecular electrostatic interactions. Although conformational changes are likely to be important for linear polyelectrolytes (e.g., charged dextrans), such effects will be largely absent for most globular proteins. Likewise, the pore size characteristics of most newer SEC resins and polymeric membranes are quite stable to changes in salt concentration. Protein adsorption is known to play a critical role in many membrane systems, and the extent of adsorption has been shown to depend on the solution pH and ionic strength [5]. Several authors have used a classical ion-exchange type model to describe 'non-ideal' retention of proteins and peptides in SEC, with the effect of ionic strength attributed to a mass-action equilibrium in which the small ions effectively 'displace' the protein from the chromatographic resin [6]. However, this type of adsorption phenomenon would be expected to be important in systems in which the protein and resin/membrane have opposite charge, while much of the SEC and UF data have actually been obtained under conditions where the protein and porous media have like charge.

Several recent studies have focused on the electrostatic exclusion of the charged proteins from the pore structure [3,7,8]. In this case, the ionic effects are assumed to be due to the alteration in the equilibrium partition coefficient between the bulk solution and the porous media caused by Debye–Hückel screening of the long-range electrostatic interactions. The equilibrium partition coefficient in this type of system can be evaluated as:

$$\phi = \frac{C_{\text{pore}}}{C_{\text{bulk}}} = \frac{1}{V}\int_{V} \exp\left(-\frac{\psi}{kT}\right) \mathrm{d}V \qquad (1)$$

where ψ/kT is the dimensionless interaction energy for the solute in the pore and V is the pore volume. ψ includes both hard sphere (excluded volume) and long-range (e.g., electrostatic) interactions between the solute and pore.

The objective of this study was to develop a more quantitative understanding of the importance of solute partitioning and electrostatic phenomena in both SEC and UF. Experimental studies of SEC and UF were thus performed in parallel using both neutral solutes (dextrans) and a charged protein (bovine serum albumin). The data were then analyzed in terms of available theoretical models for the partitioning of charged spherical solutes in cylindrical pores. The results clearly demonstrate the similarity of the electrostatic interactions in SEC and UF systems, and they provide strong support for the importance of electrostatic exclusion in determining protein partition coefficients (and in turn protein separation) in both size-exclusion chromatography and membrane ultrafiltration processes.

2. Experimental

Bovine serum albumin (BSA; Cohn Fraction V, Sigma A-7906, St. Louis, MO, USA) is a globular protein that is approximately ellipsoidal (140×40×40 Å) in shape [9]. The tertiary structure (i.e. conformation) of BSA is quite stable over a wide range of pH and ionic strength [10,11] making it attractive for use in these studies. Neutral dextrans are polymers of glucose with α-glycosidic linkages. Relatively narrow molecular mass dextran standards (19 900, 42 750, 78 800, 97 000, 165 500, 548 000 and 4 700 000) were obtained from American Polymer Standards (Mentor, OH, USA). Polydisperse dextran with a weight-average molecular mass of 67 900 was obtained from Sigma.

BSA and dextran were dissolved in either NaCl or phosphate buffer. The phosphate buffer (0.14 *M* ionic strength) was prepared by dissolving 8.04 g of $Na_2HPO_4 \cdot 7H_2O$, 4.08 g of $KH_2PO_4 \cdot H_2O$ and 0.67 g of NaOH (all from Fischer Scientific, Pittsburgh, PA, USA) in 1 l of deionized water obtained from a Barnstead (Dubuque, IA, USA) Nanopure water purification system. Higher ionic strength solutions were prepared using smaller amounts of deionized water; lower ionic strength solutions were prepared by dilution with deionized water. pH was adjusted with small amounts of 0.1 *M* HCl or NaOH as required and was measured using an Acumet 915 pH meter (Fischer Scientific, Pittsburgh, PA, USA). All salt solutions were filtered using 0.2 μm Supor membranes with a vacuum pump to remove particulates.

BSA solutions were filtered through 100 000

molecular mass cut-off polyethersulfone membranes to remove any protein oligomers and aggregates prior to use. BSA concentrations were determined using a modification of Sigma Diagnostic No. 631. This involved reaction of BSA with bromcresol green, with the BSA concentration determined from the absorbance of the resulting blue–green complex as evaluated using a Perkin-Elmer Lambda 4B UV–Vis spectrophotometer (Perkin–Elmer, Norwalk, CT, USA). Dextran concentrations were evaluated using an LC-30 refractive index (RI) detector (Perkin–Elmer, Norwalk, CT, USA). The molecular mass distribution of the polydisperse dextran was determined using SEC as described by Mochizuki and Zydney [12].

2.1. Size-exclusion chromatography

Chromatography experiments were performed using a TSK-gel G4000 SW silica resin with a hydrophilic polar (probably a glycerol–ether) bonded phase [13]. Phosphate buffer was used as the eluent at a flow-rate of approximately 0.8 ml/min. The columns were first equilibrated with fresh buffer for about an hour using at least two column volumes. This also served to flush both the sample and reference cells in the RI detector. Column equilibration was confirmed by tracking the baseline refractive index.

All samples were fed to the SEC system using an AS-400 auto-sampler (Hitachi, Columbia, MD, USA). Protein and dextran detection were both done using an LC-30 RI detector. Data collection was performed using a PE Nelson 900 Series Interface (Perkin–Elmer, Cupertino, CA, USA) connected to a Gateway 2000/386 computer. Dextran standards were run before and after each series of protein samples to verify the stability of the column.

2.2. Membrane filtration

Omega 100 000 molecular mass cut-off polyethersulfone membranes were used in the UF experiments. The membranes were initially flushed with filtered deionized water to remove any wetting agents using at least 100 l of water per m^2 membrane. The membranes were then pre-adsorbed with BSA for a minimum of 12 h prior to the experiment, using approximately 5 g/l BSA in 0.15 *M* NaCl.

The experimental procedures and results for the membrane filtration experiments are discussed by Pujar and Zydney [3]. Briefly, the data were obtained using a 25-mm diameter stirred ultrafiltration cell (Model 8010, Amicon, Division of W.R. Grace & Co., Beverly, MA, USA) connected to a 1- or 2-l solution reservoir. The transmembrane pressure drop was set by adjusting the height of the solution reservoir (for pressures less than 14 kPa) or by air pressurization. The stirring speed was adjusted using a Model 215 magnetic stirrer (Arthur H. Thomas Co., Philadelphia, PA, USA), with the actual speed evaluated using a Strobotac Type 1531-AB phototachometer (General Radio, Concord, MA, USA). Data collection was begun after the system attained stable operation, i.e. after filtration for a minimum of 2 min and after collection of a minimum of 500 μl of filtrate, with the latter required to wash out the dead volume downstream of the membrane in the stirred cell (approximately 200 μl).

Dextran sieving experiments were conducted using the polydisperse dextran with an Omega 100 000 membrane that had first been exposed to BSA for a minimum of 12 h. This preadsorption step was required to insure that the membranes used for the BSA and dextran sieving experiments had comparable pore size and surface charge characteristics. Small samples were taken from both the bulk and filtrate solutions and analyzed using size-exclusion chromatography. The chromatograms for the bulk and filtrate solution were sliced into segments covering small molecular mass fractions (approximately 1% of the dextran molecular mass) using SEC Model 2900 software (Revision 5.1, PE Nelson, Cupertino, CA, USA). The observed sieving coefficient was then evaluated from the ratio of the filtrate to bulk concentration for a particular molecular mass dextran fraction. Additional details on the dextran experiments are provided by Mochizuki and Zydney [12].

3. Results and analysis

Fig. 1 shows experimental data for the equilibrium dextran partition coefficient in the SEC resin (bottom panel) and the asymptotic dextran sieving

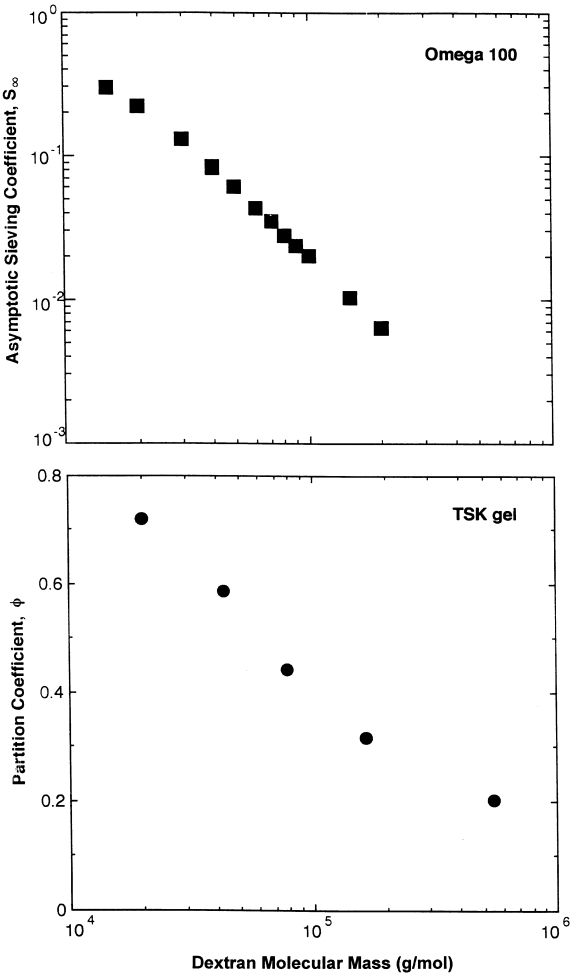

Fig. 1. Asymptotic sieving coefficient (top panel) and SEC partition coefficient (bottom panel) as a function of dextran molecular mass.

coefficient through the Omega 100 000 membrane (top panel) as a function of the dextran molecular mass. These data were all obtained at high ionic strength to minimize any electrostatic interactions associated with the charge on the SEC resin and membrane. Limited ultrafiltration experiments performed over a range of ionic strength indicated that the dextran sieving coefficients and partition coefficients were both essentially independent of the solution environment when the ionic strength was greater than 100 m*M*. The small decrease (generally less than 10%) in dextran sieving coefficients and partition coefficients at low ionic strength was due to the increase in the free energy associated with the distortion of the electrical double layer surrounding the pore wall. This is discussed in more detail subsequently. There was no evidence for any structural or conformational changes in the resin or membrane over the full range of ionic strength used in these experiments.

The dextran partition coefficient in the SEC resin was evaluated directly from the measured retention volume (V) as:

$$\phi = \frac{V - V_i}{V_{pore}} \tag{2}$$

where V_i and V_{pore} are the interstitial and pore volume, respectively. The interstitial volume was evaluated from the elution of a 4 700 000 molecular mass dextran (which was assumed to be completely excluded from the pore space) yielding $V_i = 7.61$ ml. The total void volume (equal to the pore volume plus the interstitial volume) was evaluated from the elution of a salt peak, in this case an injection of 0.14 *M* phosphate buffer into a 0.27 *M* buffer eluent. The pore volume was then evaluated as the difference between the total and interstitial volumes yielding $V_{pore} = 8.99$ ml.

The asymptotic sieving coefficient (S_∞) was evaluated from data for the dextran concentration in the permeate solution obtained as a function of filtration velocity. This required proper analysis of the effects of both bulk and membrane transport on dextran sieving as described by Mochizuki and Zydney [12]. S_∞ is equal to the dextran concentration in the permeate solution divided by the dextran concentration in the solution immediately upstream of the membrane under conditions where the solute flux through the membrane itself is governed by convection. The asymptotic sieving coefficient is directly proportional to the equilibrium solute partition coefficient between the bulk solution and the membrane pore [3,15]:

$$S_\infty = \phi K_c \tag{3}$$

where K_c is the hindrance factor for convection and accounts for the additional hydrodynamic drag on the solute molecule due to the presence of the pore wall. Theoretical analyses for an uncharged spherical solute in a cylindrical pore [16] indicate that K_c

varies from only 1.00 to 1.47, with the maximum value occurring at a solute to pore size ratio of $\lambda = 0.45$. (The values of K_c are all greater than one because of the radial variation of the velocity within the pore as discussed by Deen [15]). Thus, the variation in S_∞ seen in Fig. 1 is due almost entirely to the variation in the equilibrium partition coefficient with dextran size.

The partition coefficient and the asymptotic sieving coefficient both decrease monotonically with increasing dextran molecular mass due to the steric exclusion of the large dextrans from the region immediately adjacent to the pore wall. The dextran sieving coefficients are uniformly smaller than the SEC partition coefficients (at comparable dextran molecular mass), which is due to the much smaller effective pore size of the UF membrane used in these experiments. The smaller pore size of the UF membrane also causes a much stronger dependence of S_∞ on dextran molecular mass, with the asymptotic sieving coefficient varying by nearly two orders of magnitude while the equilibrium partition coefficient in the TSK-gel only varies by about a factor of four.

Corresponding data for the BSA partition coefficient and asymptotic sieving coefficient obtained with the same SEC resin and membrane are shown in Fig. 2 for a series of experiments performed at different solution ionic strength. The SEC data were obtained using phosphate buffer while the UF data were obtained using NaCl. (It was not possible to perform the SEC experiments with NaCl as the eluent due to the adverse effects of chloride on the column). The asymptotic sieving coefficient data show a very dramatic dependence on ionic strength, varying from $S_\infty = 0.16$ in 150 m*M* NaCl to less than 10^{-3} in the 1.5 m*M* NaCl. These data are discussed in more detail elsewhere [3]. The equilibrium BSA partition coefficient in the TSK-gel shows a somewhat weaker dependence on ionic strength due to the larger pore size of this resin, although ϕ still decreases by more than an order of magnitude as the solution ionic strength is reduced from 280 to 2.8 m*M*.

The reduction in S_∞ and ϕ seen in these experiments is most likely due to the electrostatic exclusion of the charged BSA molecules from the pores of the membrane and SEC resin, respectively. BSA has a fairly strong net negative charge at pH 7 (approximately -13 electronic charges). Both the membrane [3] and silica resin [17] are also negatively charged under these conditions, with the negative charge on the membrane arising primarily from the preferential binding of negatively-charged ions from the electrolyte solution [18]. The magnitude of the repulsive electrostatic interactions between the protein and the pore boundary will increase with decreasing ionic strength due to the reduction in electrolyte shielding provided at low salt concentrations. This increases the potential energy of interaction between the protein and the pore wall, leading to the reduction in ϕ and S_∞ seen in Fig. 2. The theoretical analysis of

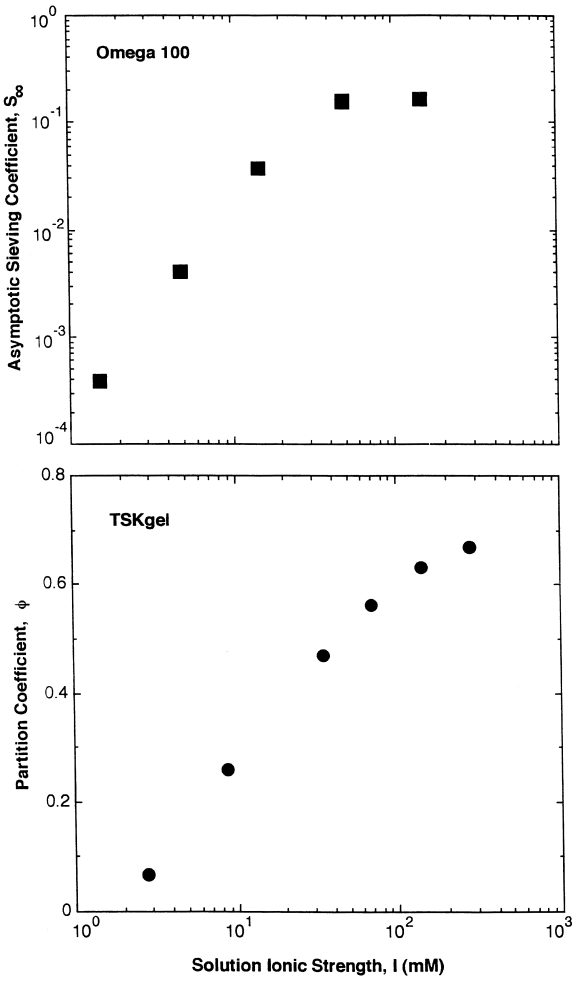

Fig. 2. Asymptotic sieving coefficient (top panel) and SEC partition coefficient (bottom panel) for bovine serum albumin at pH 7 as a function of solution ionic strength.

this phenomenon is discussed in more detail subsequently.

The experimental data in Figs. 1 and 2 can be used to evaluate the effective size of the BSA molecule in different ionic strength solutions. The effective BSA size (R_{eff}) was determined from the size of the dextran with equal sieving coefficient or partition coefficient, with the hydrodynamic radius for the particular dextran evaluated from the molecular mass as:

$$R_\eta = \left(\frac{3[\eta]M}{10\pi N_{Av}} \right)^{1/3} \quad (4)$$

where $[\eta]$ is the intrinsic viscosity, M is the dextran molecular mass, and N_{Av} is Avogadro's number. The use of the intrinsic viscosity to calculate the effective solute radius in SEC is well established [2,19]. The intrinsic viscosity of the different molecular mass dextrans was evaluated from the correlation developed by Granath [20] as:

$$[\eta] = 0.243M^{0.42} \quad (5)$$

with $[\eta]$ in cm^3/g and M in g/mol. Thus, the BSA sieving coefficient in 15 mM NaCl is equivalent to that of a 64 000 dextran yielding an effective BSA radius of 66 Å under these conditions. The results for both the SEC and UF experiments are shown in Fig. 3, with the data plotted as a function of the Debye length:

$$\kappa^{-1} = \left(\frac{F^2}{\varepsilon\varepsilon_0 RT} \sum z_i^2 C_{i\infty} \right)^{-1/2} \quad (6)$$

where F is Faraday's constant, ε_o is the permittivity of free space, ε is the dielectric constant of the bulk solution, and z_i and $C_{i\infty}$ are the valence and concentration of the electrolyte ions. The effective BSA size increases with increasing Debye length (κ) due to the reduction in both S_∞ and ϕ with decreasing ionic strength. Interestingly, the effective size data obtained from the SEC and UF experiments are nearly identical, with an approximately linear relationship between R_{eff} and κ^{-1} over this range of experimental conditions.

The similarity in the calculated values of R_{eff} from the SEC and UF experiments is actually quite surprising. In particular, the SEC resin has a significantly larger pore size than the UF membrane (as seen in the much larger values of the dextran partition coefficient compared to the S_∞ data in Fig. 1), and the porous materials are likely to have very different pore size distributions. In addition, the SEC resin and the membrane are likely to have very different surface charge characteristics (the TSK-gel is a silica-based resin while the Omega 100 000 membrane is a polyethersulfone-based material).

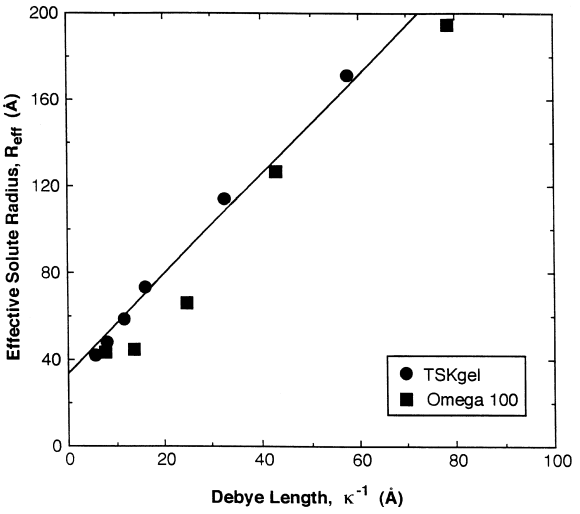

Fig. 3. Effective solute radius for BSA determined from the SEC retention time and UF sieving coefficient data as a function of the Debye length. Solid line is the theoretical prediction given by Eq. (17).

In order to examine this behavior in more detail, the effective BSA size in the different ionic strength solutions was estimated from the theoretical expression for the solute partition coefficient (Eq. (1)). In this case, the effective BSA size was evaluated as the radius of an uncharged sphere which would have the same partition coefficient as that of the charged BSA molecule in a given ionic strength solution. First, the energy of interaction for a spherical solute in a cylindrical pore was approximated as:

$$\psi = \begin{cases} \infty & \text{for } r > r_p - r_s \\ \psi_E & \text{for } r < r_p - r_s \end{cases} \quad (7)$$

where r is the radial position of the sphere center, r_s is the solute radius, and r_p is the pore radius. The electrostatic energy of interaction (ψ_E) is assumed to be constant at its centerline value yielding [15]:

$$\phi = (1-\lambda)^2 \exp\left(-\frac{\psi_E}{kT}\right) \quad (8)$$

where the pre-exponential term accounts for the steric exclusion of the spherical solute from the region within one solute radius of the pore wall (with $\lambda = r_s/r_p$). The effective solute radius can be evaluated directly from Eq. (8) as:

$$R_{eff} = r_s + (r_p - r_s)\left[1 - \exp\left(-\frac{\psi_E}{2kT}\right)\right] = r_s + (r_p - r_s)\left(\frac{\psi_E}{2kT}\right) \quad (9)$$

where the second expression is valid for sufficiently small values of the energy of interaction.

The electrostatic potential energy of interaction for a spherical solute in a cylindrical pore was evaluated by Smith and Deen [21] by solving the linearized Poisson–Boltzmann equation for the electrical potential and ion concentrations using matched expansions in spherical and cylindrical coordinates. The final results were expressed as:

$$\psi_E = A_1\sigma_s^2 + A_2\sigma_p^2 + A_3\sigma_p\sigma_s \quad (10)$$

where σ_p and σ_s are the surface charge density of the pore wall and solute, respectively, and A_1, A_2 and A_3 are all positive coefficients which depend upon the solution ionic strength, the pore radius, and the solute radius. The electrostatic energy of interaction has three distinct contributions: one associated with the distortion of the electrical double layer around the solute caused by the presence of the pore boundary (the first term in Eq. (10)), one associated with the distortion of the electrical double layer around the pore boundary caused by the entrance of the large solute into the pore (the second term), and one caused by the actual charge–charge interactions between the solute and pore [20]. Under conditions where the surface charge density of the solute is much larger than that of the pore, the energy of interaction is dominated by the first term in Eq. (10). This term is non-zero even when the pore boundary is uncharged, i.e. there is a significant increase in the free energy of the system due to the distortion of the electrical double layer surrounding the charged solute when the solute enters the pore whenever the double layer thickness is comparable to, or larger than, the spacing between the solute surface and pore boundary. Detailed calculations of the energy of interaction using available estimates for the surface charge density of the SEC resin and membrane pores confirm that the energy of interaction in these systems is dominated by the charge on the BSA molecule and is essentially independent of the charge on the pore boundary [18]. The lack of any significant dependence on σ_p is one of the underlying causes of the similarity in R_{eff} values for the SEC and UF systems. This is discussed in more detail subsequently.

The energy of interaction at the pore centerline thus becomes [21]:

$$\frac{\psi_E}{kT} = \frac{4\pi\kappa r_s^4 e^{\kappa r_s} S_o \sigma_s^2}{\varepsilon\varepsilon_0 kT(1+\kappa r_s)[\pi\kappa r_p(1+\kappa r_s)e^{-\kappa r_s} - S_o h(\kappa r_s)]} \quad (11)$$

where

$$h(\kappa r_s) = (1+\kappa r_s)e^{-\kappa r_s} - (1-\kappa r_s)e^{\kappa r_s} \quad (12)$$

The term $S_o h(\kappa r_s)$ in the denominator can be shown to be negligible under essentially all conditions. The parameter S_o is given by the integral:

$$S_o = \int_0^\infty \frac{K_1[(\kappa^2 r_p^2 + x^2)^{1/2}]}{I_1[(\kappa^2 r_p^2 + x^2)^{1/2}]}\,dx \quad (13)$$

where I_1 and K_1 are modified Bessel functions of order one of the first and second kinds, respectively. Since $K_1(z)$ decays to zero at large z while $I_1(z)$ rapidly approaches infinity, the primary contribution to the integral in Eq. (13) is in the region of small x. For moderate values of κr_p, the integral can be effectively approximated as:

$$S_o = \frac{\kappa r_p K_1[\kappa r_p]}{I_1[\kappa r_p]} \quad (14)$$

Since the electrostatic interactions are most significant at low ionic strength (i.e. small κ) and in narrow pores (small r_p), the Bessel functions in Eq. (14) can be approximated using their limiting behavior at small arguments yielding:

$$S_o = \frac{2}{\kappa r_p} \quad (15)$$

Substitution of Eq. (15) into Eq. (11) gives the following:

$$\frac{\psi_E}{kT} = \frac{8\lambda^2 r_s^2 \sigma_s^2}{\kappa\varepsilon\varepsilon_o kT} \quad (16)$$

where we have approximated the exponentials using the first terms in their Taylor series expansions. The effective solute radius is thus given as:

$$R_{eff} = r_s + \frac{4r_s^3\sigma_s^2}{\varepsilon\varepsilon_o kT}\,\lambda(1-\lambda)\kappa^{-1} \quad (17)$$

According to Eq. (17), the effective solute radius scales linearly with κ^{-1}, in excellent agreement with the results shown in Fig. 3. In addition, although R_{eff} does depend on the pore radius (through $\lambda = r_s/r_p$), the dependence on r_p is actually quite weak over a fairly broad range of pore size. For example, the function $\lambda(1-\lambda)$ only varies from 0.16 to 0.25, and then back to 0.16, as the pore radius varies from 38 to 150 Å for a solute with $r_s = 30$ Å.

The solid line in Fig. 3 represents the theoretical values of R_{eff} determined from Eq. (17) using experimental values for the BSA radius, evaluated from Eq. (4) with $[\eta] = 3.9\times10^{-6}$ m^3/g [22], and for the BSA surface charge density, evaluated from the electronic charge (−13 at pH 7) and surface area (14 700 Å^2) of the BSA molecule [3]. The calculations are shown for $\lambda(1-\lambda) = 0.2$, which is approximately the mean value over the range of $\lambda = 0.2$–0.8. The model and data are in excellent agreement. In fact, the very good agreement seen in Fig. 3 must be interpreted quite cautiously since the approximations made in the development leading to Eq. (17) are quite substantial (in particular, the use of only the first term in the Taylor series for the exponential in Eq. (9) is a poor approximation for the UF membrane due to the very large electrostatic interactions in this system). However, the theoretical results clearly indicate that the dependence of R_{eff} on κ^{-1}, as well as the similarity in the values of R_{eff} determined from the SEC and UF experiments, are in fact completely consistent with what would be expected under conditions where the electrostatic interactions are dominated by the increase in free energy associated with the distortion of the electrical double layer surrounding the BSA molecule.

The results presented in Fig. 3 indicate that two solutes with the same effective size should have identical sieving coefficients (in a given membrane) and identical SEC retention times (in a given resin), irrespective of whether that size is determined by purely steric constraints or by some combination of steric and electrostatic interactions. This is examined in more detail in Fig. 4 which shows a plot of data for the asymptotic sieving coefficients for BSA and hemoglobin (Hb) for an Omega 100 000 membrane and BSA and immunoglobulin G (IgG) for an Omega 300 000 membrane as a function of the measured retention time for the same proteins in the TSK-gel G4000SW column. The BSA data for the 100 000 membrane were taken directly from Fig. 2. The data for IgG and BSA for the 300 000 membrane were taken from Saksena and Zydney [23] in 1.5 and 150 m*M* NaCl, while the Hb data were from van Eijndhoven et al. [24] in 2.3 and 100 m*M* NaCl (all results were at a pH of approximately 7). For these latter data sets, the sieving coefficients were estimated from the minimum in the permeate concentration as a function of the filtration velocity [3], [23]. The SEC retention time was evaluated using

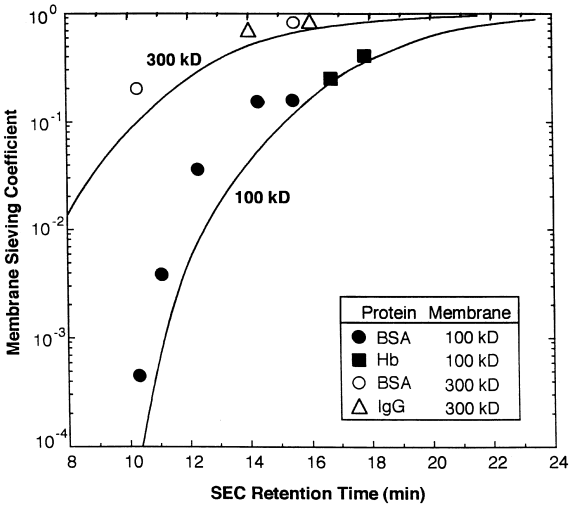

Fig. 4. Asymptotic sieving coefficient as a function of SEC retention time for bovine serum albumin (BSA), hemoglobin (Hb), and immunoglobulin G (IgG). Solid curves are results for the polydisperse dextran using the same membranes and SEC resin. kD = kilodalton.

phosphate buffer with the same pH and ionic strength as that used for the UF experiments. The solid curves in Fig. 4 are data for dextran sieving and SEC retention time obtained using the polydisperse dextran. In this case the asymptotic sieving coefficients were evaluated using Omega 100 000 and 300 000 membranes preadsorbed with BSA [14]. The retention time for the different molecular mass dextrans was evaluated from a calibration curve constructed using the data in the lower panel of Fig. 1. The good agreement between the protein data (obtained at different solution ionic strength) and the dextran data (obtained with different size molecules) clearly demonstrates the importance of both steric and electrostatic interactions on the partition coefficient in SEC and UF. It is worth noting that at high ionic strength (100 m*M*), BSA and Hb were difficult to resolve by the SEC system (resolution <0.5) and could not be effectively separated by ultrafiltration [24]. In contrast, when the solution ionic strength was reduced to 2.3 m*M*, baseline resolution was obtained using the TSK-gel G4000SW resin and high purification factors and yield were obtained using an appropriate UF diafiltration system [24]. In addition, both the SEC retention time and Omega 300 000 sieving data indicate that BSA has a smaller effective size than IgG at high ionic strength (with larger S_∞ and greater retention time), but this situation was completely reversed at low ionic strength due to the much greater negative charge on BSA than on IgG at this pH [23].

4. Discussion

The data presented in this study clearly demonstrate the importance, and underlying similarity, of steric and electrostatic interactions in determining protein retention time in SEC and protein sieving coefficients in membrane ultrafiltration. In both SEC and UF, the separation characteristics depend upon the equilibrium partition coefficient for the protein between the bulk solution and the porous media, with the magnitude of the partition coefficient determined by the combination of steric and long-range (e.g., electrostatic) interactions between the protein and the pore boundaries.

The effective protein size in both SEC and membrane systems was found to vary linearly with the Debye length, i.e. with the inverse of the square root of the solution ionic strength. This general dependence of effective size on ionic strength in SEC has been described previously by Potschka [2], [8] and among others. However, Potschka's analysis of this phenomenon focused on the specific charge–charge interactions between the protein and the pore walls (as described by the third term on the right hand side of Eq. (10)). Although such charge–charge interactions may well be important in some systems, electrostatic exclusion will also occur in SEC and UF even when the pore wall is completely uncharged due to the increase in free energy associated with the distortion of the electrical double layer surrounding the protein when the protein enters the pore. This energy penalty is completely independent of the surface charge characteristics of the pore, and it dominates the overall energy of interaction whenever σ_p is much less σ_s. The analysis presented in this paper demonstrates that when the energy of interaction is dominated by the distortion of the double layer surrounding the solute, the effective solute size will be directly proportional to the Debye length with only a weak dependence on the pore size. The combination of these two effects is the underlying cause of the similarity in the R_{eff} values determined from the SEC and UF data even though the porous media used in these experiments had very different mean pore size and different (although in both cases small) surface charge densities. The weak dependence of R_{eff} on r_p also indicates that the calculated values of R_{eff} should be largely unaffected by the presence of a pore size distribution in either the membrane or size-exclusion resin – any solute with the same effective size will have an essentially equivalent partition coefficient in each and every pore throughout the distribution. Thus, the presence of a pore size distribution should have minimal effect on the relationship between the SEC retention time (or partition coefficient) and the membrane sieving coefficient, both of which will be determined by an appropriate integral over the detailed pore size distribution.

The similarity between solute partitioning effects in SEC and UF also has important implications for process development work in membrane systems. In particular, it should be possible to use SEC retention

time data to determine optimal buffer conditions for maximizing the difference in effective size between the solutes of interest. Thus, it is possible to take advantage of the automated processing characteristics of available size-exclusion systems, as well as the small sample size required for SEC experiments, to significantly reduce the time required for development of effective high-performance membrane systems for large scale protein purification [25]. The use of SEC as part of process development for membrane systems is discussed in more detail in a future publication.

Acknowledgements

This work was supported in part by a grant from Genentech, Inc., Millipore Corp. and the Delaware Research Partnership. The authors would also like to acknowledge the helpful discussions with Robert van Reis (Genentech) and Shishir Gadam (Millipore).

References

[1] F.E. Regnier, Methods Enzymol. 91 (1983) 137.
[2] M. Potschka, J. Chromatogr. 441 (1988) 239.
[3] N.S. Pujar, A.L. Zydney, Ind. Eng. Chem. Res. 33 (1994) 2473.
[4] S.L. Edwards, P.L. Dubin, J. Chromatogr. 648 (1993) 3.
[5] A.G. Fane, C.J.D. Fell, A.G. Waters, J. Membrane Sci. 16 (1983) 211.
[6] R.R. Drager, F.E. Regnier, J. Chromatogr. 359 (1986) 147.
[7] M. Potschka, Macromolecules 24 (1991) 5023.
[8] M. Potschka, in: M. Potschka, P.L. Dubin (Eds.), Strategies in Size-exclusion Chromatography, American Chemical Society, Washington, DC, 1996, p. 67.
[9] V.L. Vilker, C.K. Colton, K.A. Smith, J. Coll. Interface Sci. 79 (1981) 548.
[10] C. Tanford, J.G. Buzzell, J. Phys. Chem. 60 (1956) 225.
[11] A.K. Gaigalas, J.B. Hubbard, M. McMurley, S. Woo, J. Phys. Chem. 96 (1992) 2355.
[12] S. Mochizuki, A.L. Zydney, J. Membrane Sci. 21 (1992) 41.
[13] K.K. Unger, J.N. Kinkel, in: P.L. Dubin (Ed.), Aqueous Size-exclusion Chromatography, Elsevier, Amsterdam, 1988.
[14] S. Mochizuki, A.L. Zydney, Biotech. Prog. 8 (1992) 553.
[15] W.M. Deen, AIChE J. 33 (1987) 1409.
[16] P.M. Bungay, H. Brenner, Int. J. Multiphase Flow 1 (1973) 25.
[17] P.J. Scales, F. Grieser, T.W. Healy, L.R. White, D.Y.C. Chan, Langmuir 8 (1992) 965.
[18] N.S. Pujar, Ph.D. Thesis, University of Delaware, 1996.
[19] P.L. Dubin, R.M. Larter, C.J. Wu, J.I. Kaplan, J. Phys. Chem. 94 (1990) 7243.
[20] K.A. Granath, J. Coll. Interface Sci. 157 (1958) 375.
[21] F.G. Smith III, W.M. Deen, J. Coll. Interface Sci. 78 (1980) 444.
[22] M.T. Tyn, T.W. Gusek, Biotech. Bioeng. 35 (1990) 327.
[23] S. Saksena, A.L. Zydney, Biotech. Bioeng. 43 (1994) 960.
[24] R.H.C.M. van Eijndhoven, S. Saksena, A.L. Zydney, Biotech. Bioeng. 48 (1995) 406.
[25] R. van Reis, S. Gadam, L.N. Frautschy, S. Orlando, E.M. Goodrich, S. Saksena, R. Kuriyel, C.M. Simpson, S. Pearl, A.L. Zydney, Biotech. Bioeng. 56 (1997) 71.